Dual-view Operational Atmospheric Correction for ATSR-2 Imagery

Peter R.J. North
Section for Earth Observation, CEH-ITE Monks Wood,
Huntingdon, Cambs PE17 2LS U.K.

ABSTRACT:

Here we describe a technique to exploit the differential atmospheric paths sampled by ATSR-2 imagery to separate the contributions from atmospheric aerosol and land surface scattering, for the solar reflective channels. The result is an image of the land surface reflectance, relatively uncontaminated by atmospheric scattering, and a separate image of the atmospheric aerosol loading. A general model of land surface bidirectional reflectance is developed and used as a constraint to simultaneously retrieve atmospheric aerosol opacity and bidirectional reflectance from top of atmosphere radiance. The inversion assumes no *a priori* knowledge of the land surface cover. The technique is demonstrated on a study of smoke aerosol over boreal forest in Canada, observed during May to September 1995. Comparison of the satellite aerosol optical thickness estimates with those derived from a ground network of solar occultation photometers show agreement to within 0.02 at 555nm, over the period. The time series of images shows greatly improved stability of the observed land surface reflectance.

Introduction

Accurate satellite observations at a global scale are required to improve understanding of the earth's radiation budget, atmospheric aerosol transport and vegetation / climate interactions (Sellers *et al* 1997). However all such observations are a mixture of contributions from the atmosphere and surface. This results in uncertainties in derived derived parameters and any intercomparison of measurements over time.

The main difficulty in atmospheric correction lies in determining the variable optical depth and scattering behaviour of aerosol particles Tropospheric aerosols significantly affect the Earth's radiation budget both due to their direct radiative effect and indirect influence on cloud formation and albedo, and atmospheric heating (Taylor and Penner 1994). They also play an important role in atmospheric chemistry and modulating the ground received UV fluxes (Andreae and P.J. Crutzen 1997).

When viewing from a single direction we must rely on the spectral signature to distinguish aerosol from ground scattering. Where a target of approximately known reflectance can be identified, such as dense vegetation or a body of water, aerosol optical depth at the target location may be estimated. However routine application is limited to regions where such targets are available at the appropriate spatial resolution, and accuracy is limited to

the level of uncertainty in the *a priori* estimate of target reflectance. For vegetation analysis the use of atmospherically resistant indices (e.g. Plummer *et al* 1994) is often preferable.

A new generation of optical sensors have the capability to acquire multiple images of the same land surface area within a short time interval, from a number of view directions (Diner *et al.* 1989, Mason and Delderfield 1990, Deschamps *et al.* 1994). These give an opportunity to further constrain atmospheric correction, to obtain estimates of aerosol scattering properties and to provide improved sampling of the angular distribution of land surface bidirectional reflectance.

Theory of dual angle correction

The reflectance the earth's surface varies not only with wavelength, but also a variation with view and illumination angle. The later has received a great deal of attention over the last decade due to the need to normalise remote sensing measurements made under a variety of viewing and illumination geometries, and with the availability of more detailed sampling of the angular domain, to use the information to improve estimates of the land surface biophysical properties.

The variation of reflectance with view angle is particularly striking over rough surfaces such as coniferous forest or ploughed fields, where reflectance may vary by a factor of five. The exact form of the angular variation is hard to predict, as it is closely tied to the three-dimensional structure of the surface imaged.

Unlike the atmospheric interaction, the land surface scattering elements are much larger than the wavelength of light, and so the geometric effects are wavelength independent. However, the inter-reflection between scattering elements and diffuse light from the atmosphere reduce the anisotropy of the land surface reflectance, as the contrast between shadowed and sunlit surfaces decreases. Considering these contributions results in a simple physical model of spectral change with view angle (North *et al* 1997),

$$r(\lambda,\Omega) = (1 - D_\lambda)P^\Omega w_\lambda + \frac{\gamma w_\lambda}{1 - g}\left(D_\lambda + g(1 - D_\lambda)\right)$$

where

$$g = (1 - \gamma)w_\lambda$$

for wavelength λ and view direction Ω.

The angular reflectance of a wide variety of natural land surfaces have been shown to fit this simple model. In contrast, reflectance that is a mixture of atmospheric and surface scattering does not fit this model well. As a result the model can be used to estimate the degree of atmospheric contamination for a particular set of reflectance measurements, and so used to find the atmospheric parameters which allow retrieval of a realistic ground reflectance (North, 1998; North *et al* 1999).

Operational implementation

Retrieval proceeds by iterative inversion of an atmospheric model on the top of atmosphere reflectance set to obtain a ground reflectance set, and testing for fit with the BRDF model. Atmospheric model inversion is performed on a local moving window of 7 by 7 km^2, within which aerosol is

assumed homogenous for the inversion. This is to minimise noise and the effect of misregistration between the two views. However reflectance retrieval is performed at the full 1km^2 resolution of the imagery. The 6S atmospheric radiative transfer model is used in the inversion, approximated by table look up for the range of conditions expected in ATSR imagery. The images are screened for cloud and for water bodies, as the strong specular reflection evident in some viewing geometries makes the inversion unreliable over water.

Results and validation

For validation and analysis, a number of ATSR-2 images were acquired over Manitoba and Saskatchewan, Canada. These coincide with the study areas of the Boreal Ecosystem-Atmosphere Study (BOREAS). The sites are dominated by coniferous forest, and provide a number of well-documented and stable study areas (Sellers *et al*, 1994).

The sites were the subject of a large scale experiment to characterise atmospheric aerosol and water vapour over the central Canada region (Markham *et al* 1997). The areas are relatively free of human sources of aerosols, but dominated by smoke aerosols from forest fires common in the summer.

Correction of smoke contaminated image
Figure 1 shows an ATSR-2 image acquired over Saskatchewan, Central Canada. The image is 512km by 512km, acquired on 25th September, 1995. A false-colour compositing scheme is used where red and green show 1630nm and 870nm nadir images respectively, while blue shows the more atmospherically sensitive 555nm along-track viewing channel. The region is dominated by wet coniferous forest in the North, and agriculture (mainly grain production) in the South. Regions of regrowth following recent fire activity are visible as red patches, due to their relatively high 1630nm reflectance. Water bodies are also visible as dark blue. The image includes the BOREAS Southern study area, which is centred on 54' N, 104' 45'' W.

The image coincides with an active forest fire located just North of the image. The smoke aerosol shows up clearly in the 555nm channel, against the relatively dark coniferous background. There is a second aerosol plume visible in the SE of the image. By contrast, the corrected image (Figure 2) shows little trace of this aerosol scattering.

Map of aerosol over BOREAS region

The aerosol optical depth at 555nm estimated throughout the 512 by 512 km region is shown in Figure 3. Values are interpolated over water bodies from estimates at the perimeter. There is a variation from 0.03 in the clear North East of the image, to 0.55 in the centre of the smoke plume.

Comparison with sun-photometer measurements

Five automatic sun-tracking radiometers were deployed during the period May to October 1995, and recorded almost continuously. The data were processed to exclude cloud contamination. The instruments were calibrated at Mauna Loa Observatory in Hawaii, with reported accuracy of ±0.02 for an air mass of 1.

Comparison with the satellite derived aerosol estimates was made for all cloud free overpasses of the sites between May and October for which simultaneous ground data was available. Aerosol optical thickness was estimated for a region of 7 by 7 km surrounding the sites, with screening of cloud contaminated pixels, and excluding dates with 20% or greater cloud contamination over the region. Values for aerosol optical thickness were interpolated for comparison at ATSR-2 wavelengths.

Figure 4 shows optical depth derived from the ATSR-2 images plotted against simultaneous measurements from the sun-photometer network. The results show rms agreement to within the .02 error bounds on the ground instruments.

Time series observations

Figures 5(a) - 5(d) show the result of atmospheric correction on a time series of observations over two of the BOREAS field sites. Figures 5(a) and 5(b) show top of atmosphere reflectance sampled by the ATSR-2 along-track channels for the northern old black spruce site and southern young jack pine sites respectively. Figures 5(c) and 5(d) show these measurements after correction. The small fluctuations remaining in the data after correction are largely explained by modelling solar/view geometry variation (North 1996).

Discussion and conclusion

A method has been described to separate atmospheric from surface scattering using the two near-simultaneous views of the ATSR-2 instrument. The method uses a simple model of land surface bidirectional reflectance to derive aerosol type and opacity, and estimate land surface bidirectional reflectance. Unlike other satellite methods for aerosol estimation, no assumptions have been made about the land surface spectral properties. Validation shows agreement between ATSR-2 optical depth retrieval and sun photometer measurements to within .02 at 555nm. An important consequence is that measurements can be compared over time and small changes in land surface reflectance resulting from changing vegetation state can be separated from atmospheric changes.

Acknowledgments

References

Sellers, P.J. *et al* (1997), Modeling the exchanges of energy, water and carbon between continents and the atmosphere, Science, 275, 502-509,.

Taylor, K.E. and Penner, J.E. (1994), Response Of The Climate System To Atmospheric Aerosols And Greenhouse Gases, Nature 369, 6483.

Andreae, M.O. and. Crutzen, P.J (1997), Atmospheric aerosols: Biogeochemical sources and role in atmospheric chemistry, Science 276, 5315.

Plummer, S.E., North, P.R.J. and Briggs, S.A. (1994) The Angular Vegetation Index (AVI): an atmospherically resistant index for the Second Along-Track Scanning Radiometer (ATSR-2), *Sixth International Symposium on Physical Measurements and Spectral Signatures in Remote Sensing*, Val d'Isere.

Diner, D.J. *et al.* (1989) MISR: A multiangle imaging spectroradiometer for geophysical and climatological research for EOS. IEEE Trans. Geosci. Remote Sens., vol. 27, pp. 200-214.

Mason, I. and Delderfield, J. (1990), Scientific requirements specification for the ATSR-2 on ERS-2. *Rutherford-Appleton Laboratories Technical Report* ER-RS-MSL-AT-2001.

Deschamps, P.-Y. *et al* (1994), The POLDER mission: instrument characteristics and scientific objectives, . IEEE Trans. Geosci. Remote Sens., vol. 32, pp. 598-615.

North, P.R.J., Briggs, S.A., Plummer, S.E. and Settle, J.J. (1997), Development of novel algorithms for atmospheric correction of ATSR-2 dual angle imagery, *in Proc. of the Seventh International Symposium on Physical Measurements and Signatures in Remote Sensing*, Courchevel, France. 7-11th April.

North, P.R.J. (1988) Dual-view operational atmospheric correction for ATSR-2 imagery, *Proc. of International Geoscience and Remote Sensing Symposium*, 6-10 July, Seattle Washington, USA.

North, P.R.J., Briggs, S.A., Plummer, S.E. and Settle, J.J. (1999), Retrieval of land surface bidirectional reflectance and aerosol opacity from ATSR-2 multi-angle imagery, IEEE Trans. Geosci. Remote Sensing, vol. 37, No.1.

Vermote, E.F., Tanre, D., Deuze, J.L., Herman, M and Morcrette, J.J. (1997) Second Simulation of the Satellite Signal in the Solar Spectrum, 6S: An overview, IEEE Trans. Geosci. Remote Sensing 35, 3.

Sellers, P.J. et al, (1994) Experiment plan: Boreal Ecosystem-Atmosphere Study, version 3.0, NASA Goddard Space Flight Cent., Greenbelt, Md.

Markham, B.L., Schafer, J.S. Holben, B.N. and Halthore, R.N. (1997), Atmospheric aerosol and water vapour characteristics over north central Canada during BOREAS, J. Geophys. Res. 102, D24.

North, P.R.J. (1996) Three-dimensional forest light interaction model using a Monte Carlo method, IEEE Trans. Geosci. Remote Sensing, Vol. 34, No. 5, pp. 946-956.
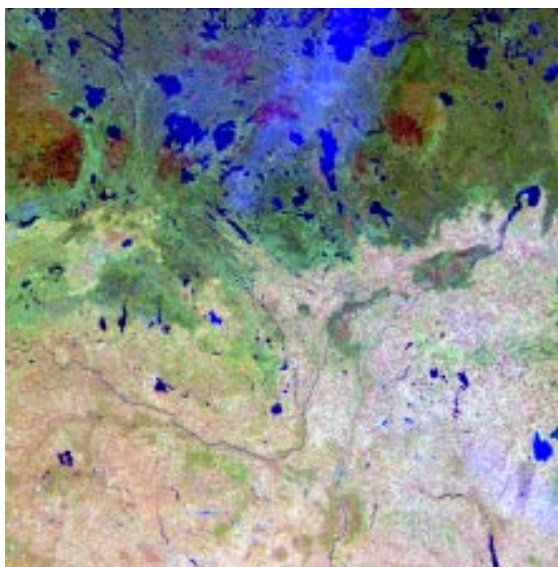
Figure 1. Saskatchewan Canada, top of atmosphere colour composite; red: 1630nm, green: 870nm, blue 555nm. The image shows coniferous forest to the north and agricultural crops in the south. Strong aerosol scattering is visible in the north of the image, and in the south-east.
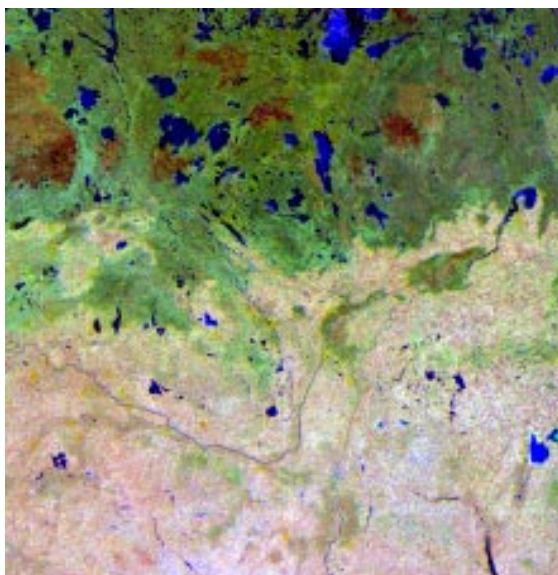

Figure 2. Saskatchewan Canada, surface reflectance colour composite; red: 1630nm, green: 870nm, blue 555nm. The dual-view technique has been used to separate the atmospheric contribution from the land surface, leaving the image relatively free of aerosol contamination.
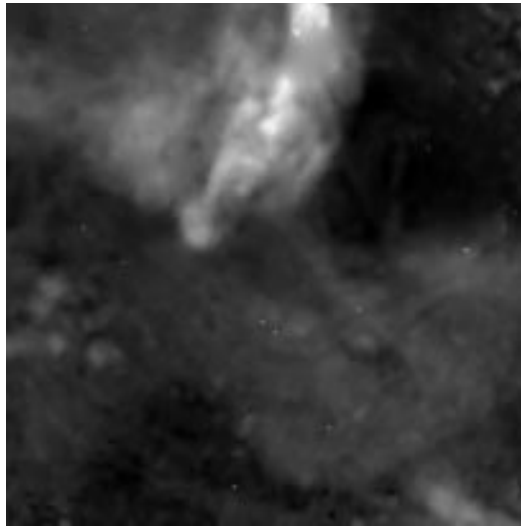
Figure3. Image of aerosol optical thickness (range 0-0.6) retrieved over ATSR-2 image
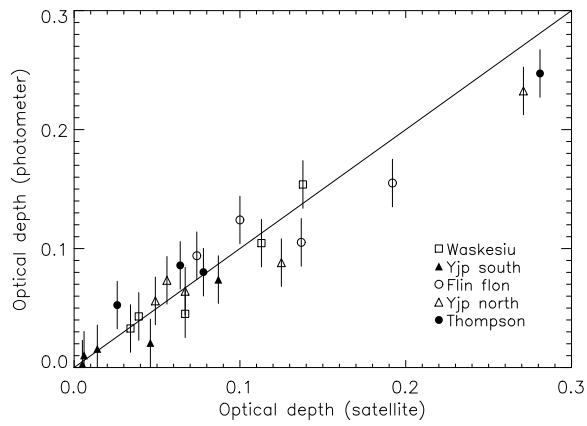
Figure 4. Comparison of satellite derived aerosol optical thickness at 555nm with measurements from ground BOREAS network of sun photometers, May -October 1995.
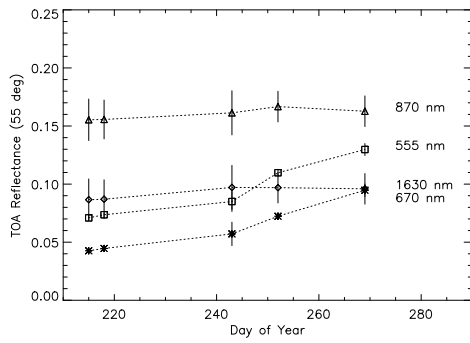
Figure 5(a). Top of atmosphere time series, northern BOREAS old black spruce site sampled by the ATSR-2 along-track view.
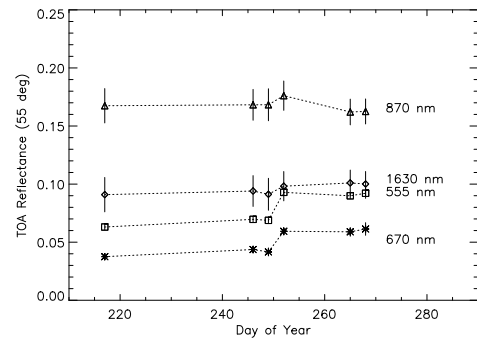

Figure 5(b). Top of atmosphere time series, southern BOREAS young jack pine site sampled by the ATSR-2 along-track view.
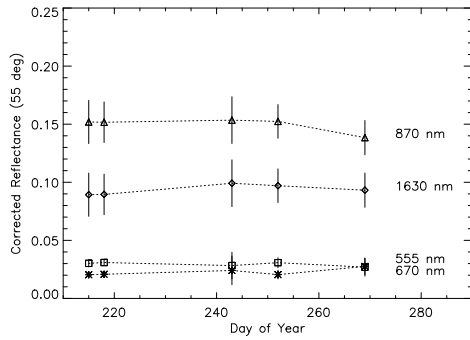

Figure 5(c). Atmospherically corrected series, northern BOREAS old black spruce site.
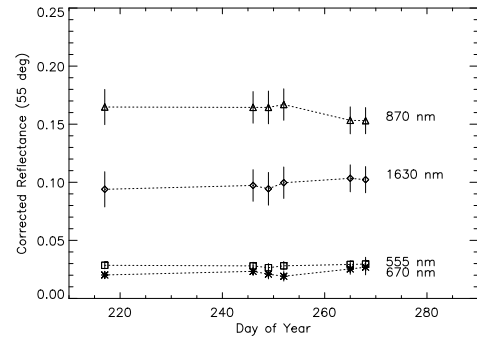
Figure 5(d). Atmospherically corrected series, southern BOREAS young jack pine site.